

Supporting information for: Physisorption of bio oil nitrogen compounds onto montmorillonite

Maisa Vuorte,[†] Susanna Kuitunen,[‡] and Maria Sammalkorpi^{*,†,¶}

[†]*Department of Chemistry and Materials Science, School of Chemical Engineering, Aalto University, P.O. Box 16100, FI-00076 Aalto, Finland*

[‡]*Neste Engineering Solutions Oy, P.O. Box 310, FI-06101 Porvoo, Finland*

[¶]*Department of Bioproducts and Biosystems, School of Chemical Engineering, Aalto University, P.O. Box 16100, FI-00076 Aalto, Finland*

E-mail: maria.sammalkorpi@aalto.fi

Supporting information

The supporting information consists of the bootstrapped PMF profiles (Figure 1) and PMF curve decomposition into Coulombic and Lennard-Jones contributions (Figure 2) for imidazole, as well as the partial charge decomposition of the N-heterocycles (Figures 3 and 4) and fatty acid amides (Figure 5) derived from the single point DFT calculations. For further computational details, refer to Section 2.2 of the main article.

Bootstrapped PMF profiles for imidazole

The average PMF profiles were calculated based on a bootstrap method using 300 bootstrap samples for each set of umbrella sampling simulations. The profiles were overlapped by setting the zero level of each generated PMF profile at $r = 2.05$ nm. The PMF profiles presented in Figures 2 and 4 of the main manuscript are based on the arithmetic average of the bootstrapped profiles and error is estimated using standard deviation. To present the data fluctuations range and PMF convergence, Figure 1 plots the sampled 300 bootstrapped profiles for imidazole.

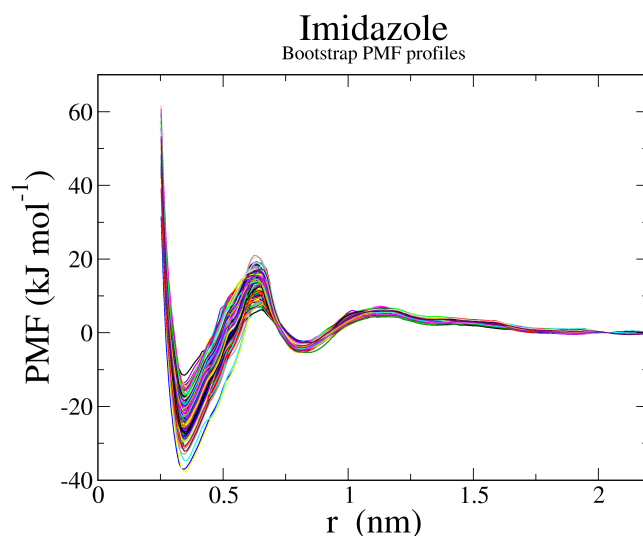


Figure 1: 300 bootstrapped PMF profiles for imidazole. PMF reaction coordinate r denotes perpendicular distance between the montmorillonite surface topmost Si atoms and imidazole molecule center of mass.

Imidazole PMF decomposition to Coulombic and van der Waals non-bonded contributions

Adsorption of the examined heterocycles occurs via interaction with the montmorillonite surface Na^+ ions. It is worthwhile posing the question, how the adsorption contributions

depend on Coulombic and van der Waals contributions.

Figure 2 shows the contributions of Lennard-Jones (LJ) and Coulombic non-bonded interactions to the overall PMF of imidazole. To obtain the data, additional PMF umbrella sampling simulations for imidazole on montmorillonite with electrostatic (Coulombic) interactions between the imidazole molecule and the rest of the system (triglyceride solvent and montmorillonite surface and ions) turned off were performed. Imidazole intramolecular electrostatic interactions and interactions between the solvent molecules, montmorillonite atoms and Na^+ ions were kept intact. The PMF was calculated according to the protocol described in main manuscript. The electrostatic contribution to the PMF was calculated by subtracting the simulated LJ contribution from the original PMF. Notably, a PMF in which the electrostatic interactions between the species of interest, here imidazole, and the rest of the system are turned off, converges significantly faster, as e.g. hydrogen bonding interactions between the triglyceride solvent and imidazole are absent.

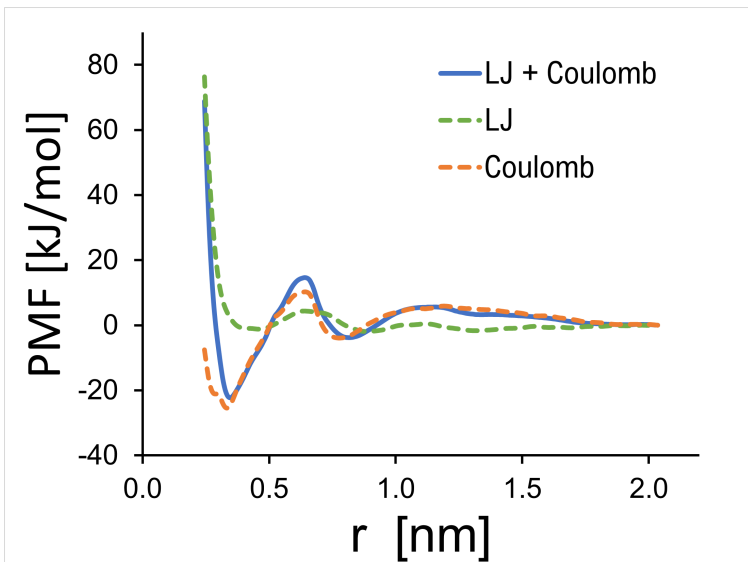


Figure 2: PMF profile for imidazole adsorbing onto Na-montmorillonite as the function of distance r to the plane defined by Montmorillonite surface Si atoms. Contributions arising from Lennard-Jones (LJ) and Coulombic interactions are plotted separately.

During umbrella sampling the imidazole molecule is confined only in the z -direction (perpendicular to the montmorillonite surface), which allows movement along the xy -plane on the

montmorillonite surface. In the absence of Coulombic interactions, the adsorption geometry changes. This shows in the small r PMF data corresponding to just the LJ contributions.

The data of Figure 2 supports the conclusion that the contribution of LJ-interactions to adsorption is much smaller than the Coulomb interaction contributions. This means that the overall adsorption energy can be expected to scale with molecule point charges, particularly the adsorbing imidazole ring nitrogen. Imidazole is employed as the test case here due to its two ring nitrogens.

Partial charges of N-heterocycles and fatty acid amides

The original Charmm GenFF charges,¹ as well as Hirshfeld,² AIM,³ Merz-Singh-Kollman (MK),^{4,5} and ChelpG⁶ charges of the studied nitrogen compounds are presented in Figures 3, 4, and 5. The mean, median, and standard deviation of the absolute error for each charge partition scheme compared to Charmm GenFF charges are also presented.

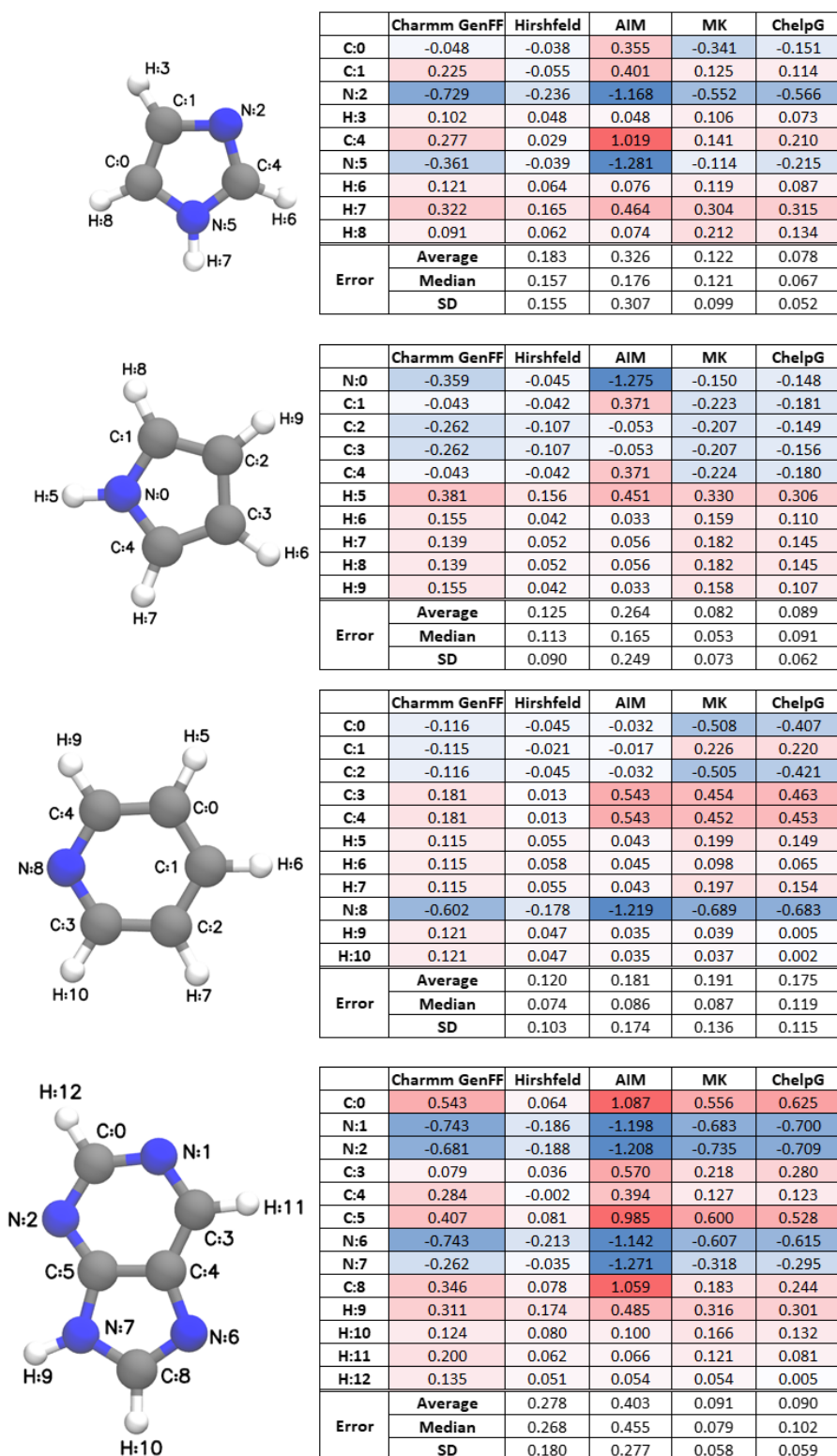
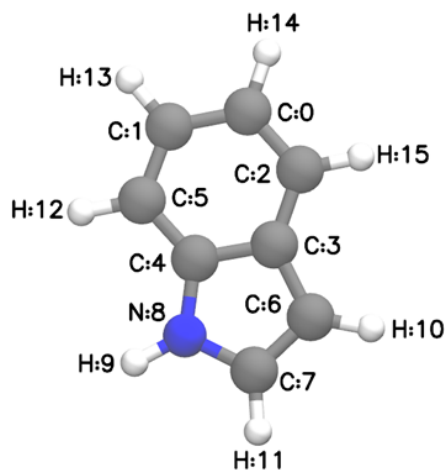
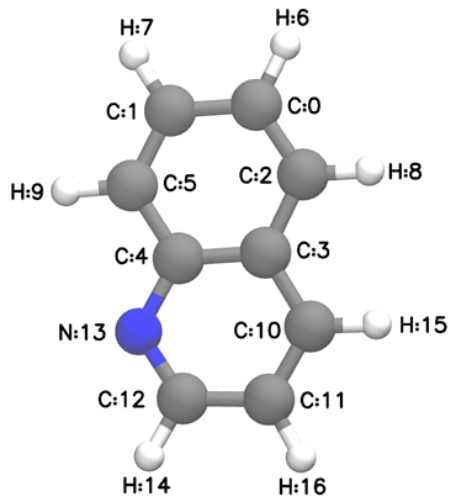


Figure 3: The Charmm GenFF partial charges and the DFT calculation based Hirshfeld, AIM, Merz-Singh-Kollman (MK), and ChelpG charges of imidazole, pyrrole, pyridine, and purine. The charge unit is elementary charge. The average, median, and standard deviation (SD) of absolute error in comparison to Charmm GenFF charges are also presented.



	Charmm GenFF	Hirshfeld	AIM	MK	ChelpG
C:0	-0.214	-0.068	-0.034	-0.143	-0.047
C:1	-0.180	-0.062	-0.029	-0.144	-0.136
C:2	-0.246	-0.055	-0.025	-0.356	-0.334
C:3	0.145	-0.039	-0.029	0.302	0.284
C:4	0.235	0.021	0.392	0.183	0.099
C:5	-0.277	-0.066	-0.021	-0.339	-0.226
C:6	-0.248	-0.101	-0.045	-0.496	-0.391
C:7	-0.082	-0.014	0.384	-0.146	-0.113
N:8	-0.487	-0.052	-1.269	-0.277	-0.254
H:9	0.360	0.157	0.455	0.331	0.307
H:10	0.183	0.047	0.043	0.230	0.169
H:11	0.170	0.060	0.065	0.206	0.172
H:12	0.192	0.047	0.030	0.188	0.141
H:13	0.124	0.042	0.021	0.141	0.102
H:14	0.124	0.040	0.018	0.135	0.076
H:15	0.201	0.045	0.025	0.186	0.152
Error	Average	0.164	0.217	0.073	0.080
	Median	0.146	0.168	0.049	0.051
	SD	0.083	0.169	0.070	0.063



	Charmm GenFF	Hirshfeld	AIM	MK	ChelpG
C:0	-0.114	-0.043	-0.022	-0.198	-0.114
C:1	-0.112	-0.039	-0.023	-0.084	-0.018
C:2	-0.116	-0.041	-0.023	-0.159	-0.203
C:3	-0.005	-0.011	-0.020	-0.173	-0.027
C:4	0.375	0.036	0.460	0.741	0.560
C:5	-0.129	-0.047	-0.023	-0.400	-0.329
H:6	0.115	0.051	0.035	0.161	0.108
H:7	0.115	0.052	0.036	0.154	0.097
H:8	0.115	0.051	0.034	0.150	0.137
H:9	0.115	0.048	0.048	0.182	0.148
C:10	-0.116	-0.019	-0.017	0.030	-0.016
C:11	-0.115	-0.048	-0.033	-0.439	-0.328
C:12	0.155	0.021	0.605	0.392	0.409
N:13	-0.634	-0.173	-1.203	-0.754	-0.701
H:14	0.121	0.049	0.036	0.065	0.023
H:15	0.115	0.058	0.045	0.139	0.114
H:16	0.115	0.055	0.044	0.193	0.142
Error	Average	0.109	0.130	0.125	0.084
	Median	0.071	0.085	0.078	0.067
	SD	0.111	0.141	0.107	0.080

Figure 4: The Charmm GenFF partial charges and the DFT calculation based Hirshfeld, AIM, Merz-Singh-Kollman (MK), and ChelpG charges of indole and quinoline. The charge unit is elementary charge. The average, median, and standard deviation (SD) of absolute error in comparison to Charmm GenFF charges are also presented.

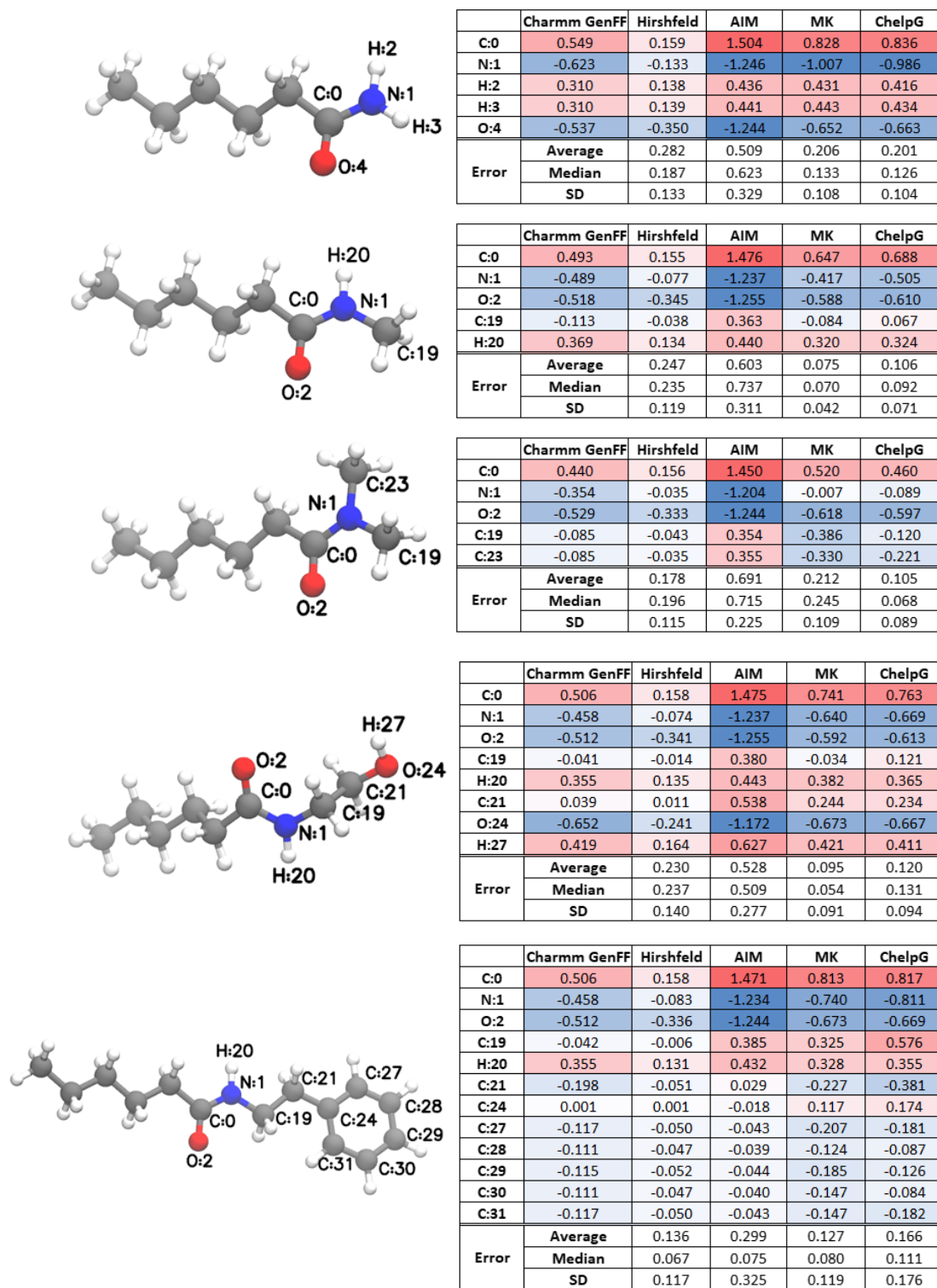


Figure 5: The Charmm GenFF partial charges and the DFT calculation based Hirshfeld, AIM, Merz-Singh-Kollman (MK), and ChelpG charges of the studied fatty acid amides. The charge unit is elementary charge. The average, median, and standard deviation (SD) of absolute error in comparison to Charmm GenFF charges are also presented.

References

- (1) Vanommeslaeghe, K.; Hatcher, E.; Acharya, C.; Kundu, S.; Zhong, S.; Shim, J.; Darian, E.; Guvench, O.; Lopes, P.; Vorobyov, I., et al. CHARMM general force field: A force field for drug-like molecules compatible with the CHARMM all-atom additive biological force fields. *Journal of computational chemistry* **2010**, *31*, 671–690.
- (2) Hirshfeld, F. L. Bonded-atom fragments for describing molecular charge densities. *Theoretica chimica acta* **1977**, *44*, 129–138.
- (3) Bader, R. F. Atoms in molecules. *Accounts of Chemical Research* **1985**, *18*, 9–15.
- (4) Singh, U. C.; Kollman, P. A. An approach to computing electrostatic charges for molecules. *Journal of computational chemistry* **1984**, *5*, 129–145.
- (5) Besler, B. H.; Merz Jr, K. M.; Kollman, P. A. Atomic charges derived from semiempirical methods. *Journal of computational chemistry* **1990**, *11*, 431–439.
- (6) Breneman, C. M.; Wiberg, K. B. Determining atom-centered monopoles from molecular electrostatic potentials. The need for high sampling density in formamide conformational analysis. *Journal of Computational Chemistry* **1990**, *11*, 361–373.